

Relations between ^{77}Se NMR chemical shifts of (phenylseleno)-benzenes and their molecular structures derived from nine X-ray crystal structures

Jette Oddershede,^a Lars Henriksen^b and Sine Larsen^{*a}

^a Centre for Crystallographic Studies, Department of Chemistry, University of Copenhagen, Universitetsparken 5, DK-2100 Copenhagen O, Denmark. E-mail: sine@ccs.ki.ku.dk; Fax: +45 3532 0299; Tel: +45 3532 0282

^b Laboratory of Organic Chemistry, Department of Chemistry, University of Copenhagen, Universitetsparken 5, DK-2100 Copenhagen O, Denmark

Received 27th November 2002, Accepted 23rd January 2003

First published as an Advance Article on the web 21st February 2003

An extensive library of ^{77}Se chemical shifts have been generated from the NMR measurements on substituted (phenylseleno)benzenes, including 33 new compounds. The variation in chemical shifts cover 265 ppm ranging from 446 to 181 ppm.

Crystal structures have been determined for nine selected representatives of the substituted (phenylseleno)-benzenes. The analysis of the crystal structures supported that through-space interactions between selenium and the *ortho*-substituent observed in the crystal structures also are likely to be present in solution.

The variation in the ^{77}Se NMR chemical shifts can be rationalised from the intramolecular interactions with the substituent in the *ortho*-position. Furthermore it appears that these *ortho*-effects are roughly additive, and that it is the actual interactions and not the resulting conformational constraints that are responsible for the variations in the ^{77}Se NMR chemical shifts.

Introduction

Previous studies of ^{77}Se chemical shifts in 4,4'-disubstituted diaryl selenides¹ and *m*- and *p*-substituted selenoanisoles,^{2,3} have indicated that the ^{77}Se chemical shifts are influenced by polar effects. A Hammett correlation with a positive ρ value (deshielding by electron attracting-, shielding by electron donating groups) was proposed in both series. The variations of the observed chemical shifts cover 62 ppm (4,4'-dinitro- to 4,4'-diaminodiphenyl selenide) in the diaryl selenides and 52 ppm (4-nitro- to 4-(dimethylamino)selenoanisole) in the selenoanisoles. In the latter series it was noted that *ortho*-substituted compounds behave anomalously, and as possible causes for this anomaly the authors suggested conformational constraints to the phenylseleno group and/or through-space interaction with the *ortho*-substituent.⁴

We have routinely used ^{77}Se NMR shifts as a documentary parameter as part of our studies of the electrophilic^{5,6} and nucleophilic⁷ phenylselenylation of arenes. During these investigations it became apparent that the ^{77}Se NMR chemical shifts of the *o*-substituted (phenylseleno)benzenes exhibit even larger variations than those previously reported,¹⁻³ and are greatly affected by the nature of the substituents. In order to elucidate this aspect further we have prepared 33 new differently substituted (phenylseleno)benzenes, all represented by the general structure shown in Fig. 1. The ^{77}Se NMR chemical shifts recorded for these compounds show great variations with the different substituents labelled by a, b, c, a', b'. Together

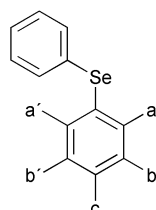


Fig. 1 The (phenylseleno)benzene unit showing the labelling for the positions of the substituents.

with the previously obtained results, these new δ values have given us an extensive library of chemical shifts in substituted (phenylseleno)benzenes.

We present here the preparations of 33 new (phenylseleno)benzenes and the compilation of the ^{77}Se chemical shifts in this type of compounds. The information contained in this library has been used as the basis for an analysis of the relations between the ^{77}Se NMR chemical shifts and the nature and positions of the substituents. To elucidate the structural origins for the significant variations observed in the chemical shifts, X-ray structure determinations were conducted for the nine representative compounds, covering combinations of *o*-methyl-, -methoxy (-OMe), -hydroxy, and -phenylseleno (-SePh) substituents, shown in Fig. 2. These structure determinations made it possible for us to investigate the influence of the phenylseleno substituent on the geometry of the benzene ring, reflected in the deviation of the angles from the idealised 120°.

Results and discussion

Preparations

The substituted (phenylseleno)benzenes were prepared from the appropriate arenes by electrophilic substitution using the *ortho*-specific reagent couple diphenyl diselenide–benzeneseleninic acid⁵ for *ortho*-substitution of phenols, and the *para*-selective reagent couple diphenyl diselenide–dihydroxyphenylselenonium tosylate⁶ in all other cases.

^{77}Se NMR chemical shifts

A compilation of a total of 45 ^{77}Se NMR shifts recorded from mono-, bis- and tris(phenylseleno)arenes is contained in Table 1. The substituent denominations refer to Fig. 1 and the entries are sorted according to decreasing chemical shift (δ) values. This organizing system means that some bis- and tris(phenylseleno) compounds appear under more than one entry. The regiochemistry is, of course, well established for the compounds that have been subjected to crystal structure

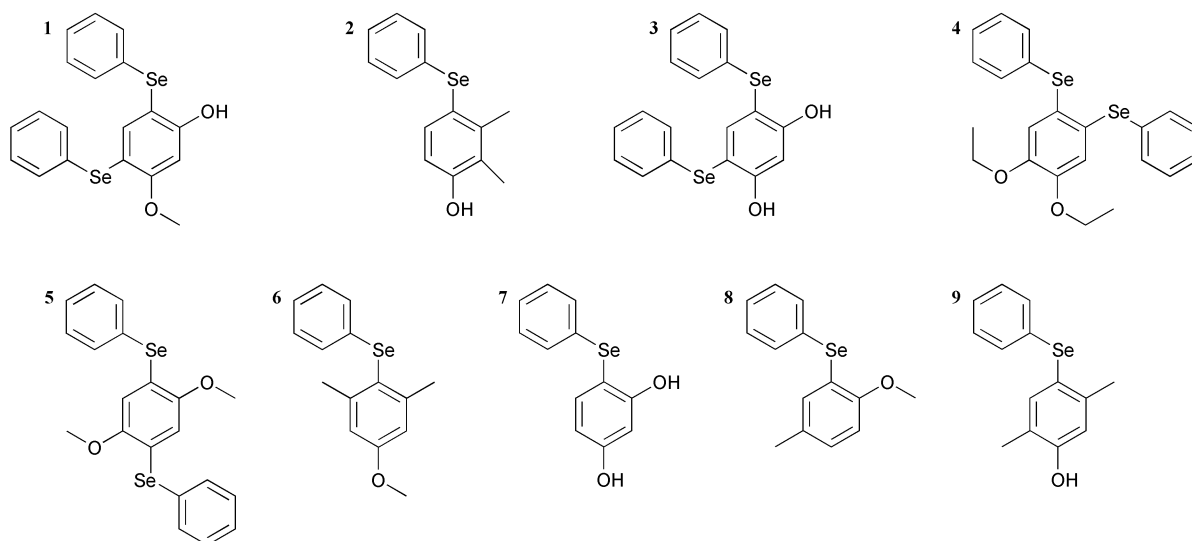


Fig. 2 The nine compounds that were selected for crystal structure determination.

Table 1 ^{77}Se NMR chemical shifts of (phenylseleno)benzenes

	a	a'	b	b'	c	δ/ppm	
1	H	H	H	H	NO_2	446	
2	H	SePh	Me	Me	OMe	445	
3	H	H	COOH	SePh	OH	427	
4	SePh	H	H	OEt	OEt	425	
5	H	H	H	H	H	422	
6	H	H	Br	H	OMe	420	
7	H	H	H	CHO	OH	417	
8	H	H	H	SePh	OH	416	
9	Cl	H	H	SePh	OH	411	
10	H	H	H	Me	OH	409	
11	H	H	Me	Me	OH	409	
12	H	H	H	H	OMe	409	
13	H	H	H	H	OH	407	
14	H	H	H	Me	OH	407	
15	Cl	H	H	H	OH	403	
16	OMe	H	H	Br	H	382	
17	OH	H	COOH	SePh	H	379	
18	2	Me	H	Me	OH	378	
19	5	OMe	H	H	OMe	SePh	374
20	8	OMe	H	H	Me	H	363
21	Me	Me	SePh	SePh	OH	361	
22	Me	SePh	OMe	H	Me	354	
23	OMe	H	H	SePh	OMe	352	
24	1	OMe	H	H	SePh	OH	350
25	9	Me	H	H	Me	OH	345
26	OMe	H	H	H	OMe	343	
27	OH	H	SePh	COOMe	H	327	
28	Me	Me	H	SePh	OH	326	
29	OH	H	SePh	H	H	322	
30	6	Me	Me	H	H	OMe	291
31	Me	Me	H	H	OH	290	
32	OH	Me	SePh	SePh	Me	288	
33	OH	H	H	SePh	Cl	264	
34	OH	H	H	COOMe	H	263	
35	OH	H	H	Me	H	259	
36	OH	H	H	SePh	H	257	
37	OH	H	H	H	H	257	
38	OH	H	Me	H	H	256	
39	OH	H	H	H	Cl	254	
40	OH	Me	SePh	H	Me	253	
41	3	OH	H	H	SePh	OH	248
42	1	OH	H	H	SePh	OMe	248
43	7	OH	H	H	H	OH	240
44	OH	Me	H	SePh	Me	213	
45	OH	Me	H	H	Me	181	

determination (1–9). Assignments for the remaining compounds are in accord with the mechanistic principles previously discussed^{5,6} and supported by the chemical shifts and coupling patterns in the ^1H NMR spectra (*cf.* Experimental section).

The ^{77}Se chemical shifts listed in Table 1 range from 446 to 181 ppm, and it is apparent that amendments are needed to the straightforward dependence on polar effects. In particular the effect of *ortho*-substituents, covering a chemical shift range of 260 ppm, by far exceeds those exerted by the *meta*- and *para*-substituents. Compounds that do not have any substituents in an *ortho*-position to selenium display δ values in the 446–407 ppm range. An *o*-Me or *o*-OMe substituent displaces the δ values to the range 382–343 ppm, *i.e.* by about –60 ppm, and an *o*-OH substituent generally to the range 264–240 ppm, *i.e.* by about –160 ppm. These *ortho*-effects are roughly additive. Thus two *o*-Me groups give a shift of about –120 ppm (entries 30, 31) and the combination of an *o*-Me and an *o*-OH group a shift of about –220 ppm (entries 44, 45). All three types of *ortho*-substitution lead to chemical shifts well outside the range for compounds with hydrogen in both *ortho*-positions. This fact establishes ^{77}Se NMR shifts as an efficient analytical tool for determining regiochemical relations. Further elucidation of this aspect requires detailed structural information obtainable from the crystal structures.

Crystal structures †

ORTEP II drawings depicting the molecular structures of the nine compounds,⁸ determined by X-ray diffraction methods, are displayed in Fig. 3. It should be noted that one of the compounds (7) crystallizes with two molecules in the asymmetric unit and that 5 exploits its molecular symmetry and crystallizes with the molecule on a crystallographic inversion centre. Since it is our aim to correlate molecular structures found in the crystalline state with ^{77}Se NMR chemical shifts measured on solutions, our first goal is to inspect and analyse the structures in order to identify any structural features that could be perturbed by the crystal packing. The program PLATON was used for the identification and calculation of both inter- and intramolecular close contacts.⁹

Crystal packing. The crystal packing in all nine structures displays the common feature of layers of weakly interacting stacked phenyl groups. The packing of compound 7 in Fig. 4 is shown as a representative example. Molecules without the possibility of hydrogen bond interactions show a crystal packing that is determined by the weak interactions within and between the layers of phenyl groups. This is the packing mode seen for compounds 1, 4, 5, 6 and 8. The remaining four

† CCDC reference numbers 197542–197550. See <http://www.rsc.org/suppdata/ob/b2/b211130f/> for crystallographic data in .cif or other electronic format.

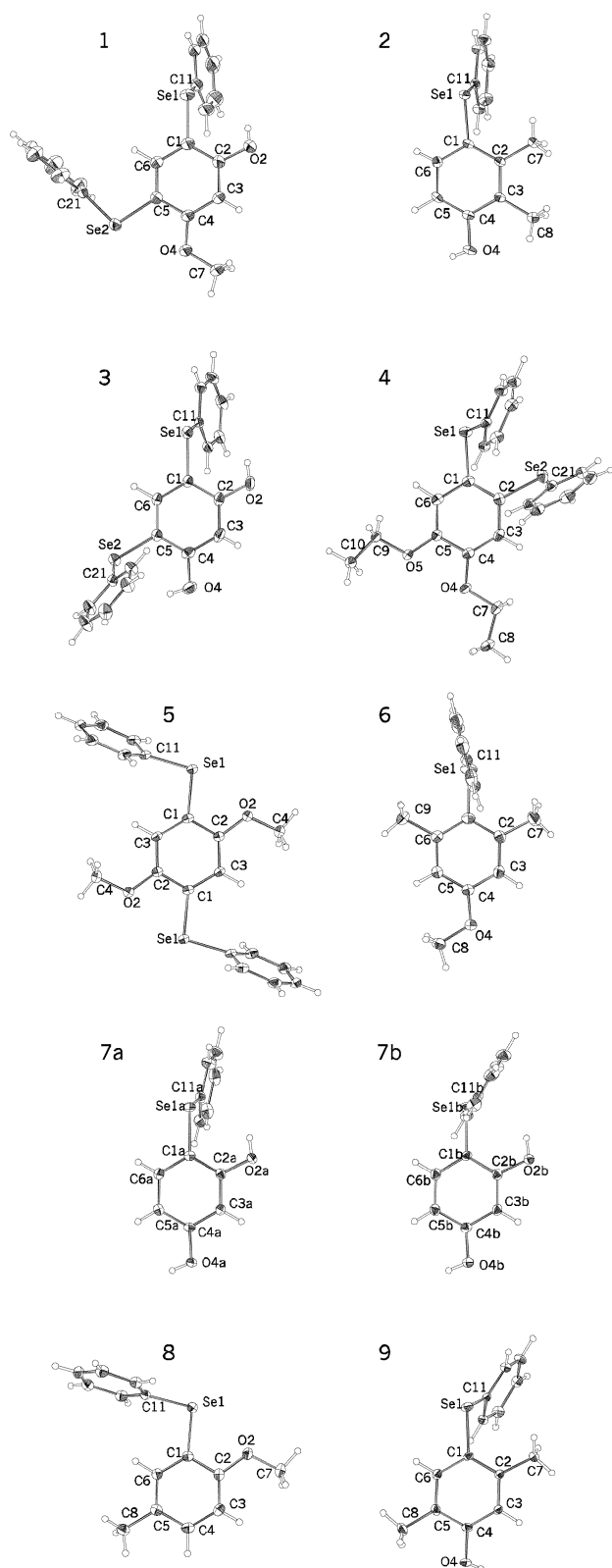


Fig. 3 ORTEP II drawings showing the atomic labelling of 1–9. The thermal ellipsoids are drawn to include 50% probability, and the hydrogen atoms as spheres with a fixed radius.

compounds contain hydroxy groups that have the possibility of hydrogen bond formation. Significant intermolecular interactions are listed in Table 3.

Only one of the compounds with two hydroxy groups (**7**) forms hydrogen bonds between hydroxy groups. The result is a complicated pattern of O–H...O hydrogen bonds with O...O distances in the range 2.76–2.90 Å, see Fig. 5. O4 from each of the two independent molecules (**7a** and **7b**) is linked by

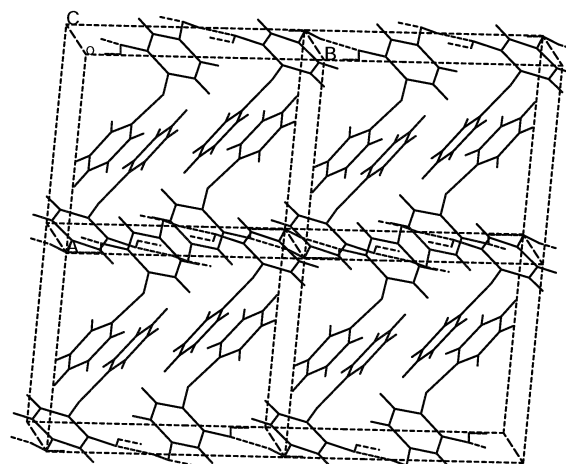


Fig. 4 Cerius² view of the crystal packing in **7**.¹⁷

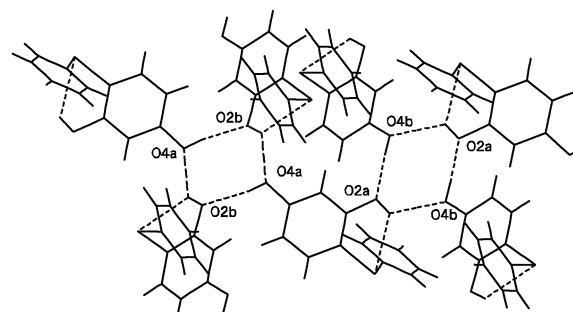


Fig. 5 Cerius² drawing of the hydrogen bonds in compound **7**.¹⁷ The atomic labelling is the same as on Fig. 3.

a perfect linear hydrogen bond to O2 of the other independent molecule forming chains of molecules along the crystallographic *b*-axis. In addition, in the direction of the *c*-axis, O2a is linked to O4b and O2b to O4a, integrating the molecules into four-membered hydrogen bonded rings. The ring connecting O2a and O4b is almost identical to the one connecting O2b and O4a. The geometries of the O2–H2...O4 intermolecular interactions suggest that these are part of a three-center hydrogen bond system, and indeed an intramolecular O2–H2...Se1 hydrogen bond completes the system in both molecules. The O2...Se1 distances are 3.15 and 3.17 Å for **7a** and **7b**, respectively, and the O2–H2...Se1 angles are just above 123°.

The two independent molecules in the asymmetric unit of compound **7** differ with respect to the orientation of the phenyl ring relative to the benzene ring. Since the hydrogen bonds of the two molecules are so alike, they cannot be the reason for this difference in the molecular geometry, so perhaps the reason should be sought in the crystal packing. Most likely the crystallization of compound **7** starts out with identical molecules assembling in the hydrogen bonding pattern of Fig. 5 in the *bc*-plane. In the direction of the *a*-axis weak phenyl–phenyl interactions are responsible for the stacking of the layers. The twisting of some of the phenyl groups that leads to conformational differences between the two independent molecules in **7** may be necessary to obtain favourable stacking interactions in this direction. The assumption of fast growing layers parallel to the *bc*-plane in which the molecules are connected by hydrogen bonds, and much weaker interactions along the *a*-axis is supported by the fact that the crystals are plates with (100) as the plate face.

The ability of a phenylseleno group to be the proton acceptor in an intramolecular hydrogen bond, as observed in compound **7**, is also exploited in the crystal packing of compounds **2** and **9**. These structures contain intermolecular O4–H4...Se1 contacts where the hydroxy group forms a perfect two-centre hydrogen bond to the selenium atom with O...Se distances

Table 2 Selected bond lengths (Å), angles (°) and torsion angles (°)

	a	Se–C1	Se–C11	C1–Se–C11	Se–C1–C2	C1–C2–a	Se–C1–C2–a	C2–C1–C11	C1–Se–C11–C12
1	OH	1.912(2)	1.916(3)	101.36(13)	120.38(18)	123.3(2)	–4.9(5)	82.9(3)	–9.6(2)
	OMe	1.917(2)	1.930(3)	99.50(10)	117.00(18)	115.7(2)	2.6(4)	–162.1(2)	79.3(2)
2	Me	1.9210(19)	1.9284(19)	101.51(8)	122.76(14)	122.03(17)	–5.6(2)	78.19(16)	7.27(18)
3	OH	1.907(3)	1.921(3)	101.10(11)	120.4(2)	122.5(3)	–4.5(4)	77.9(2)	–5.2(2)
	OH	1.910(3)	1.925(3)	100.93(11)	120.3(2)	121.7(3)	–4.0(4)	71.7(2)	18.7(3)
4	SePh	1.924(3)	1.917(3)	99.22(12)	123.1(2)	122.6(2)	–2.8(3)	–105.0(2)	0.6(3)
	SePh	1.921(3)	1.927(3)	98.95(12)	122.6(2)	123.1(2)	–2.8(3)	–67.5(3)	–28.9(3)
5	OMe	1.920(2)	1.919(2)	101.80(10)	114.67(18)	115.0(2)	1.2(3)	176.16(17)	79.3(2)
6	Me Me	1.9270(17)	1.9177(17)	100.49(7)	119.35(13)	122.61(17)	4.9(2)	–94.19(14)	15.82(16)
					119.70(12)	122.36(15)	–4.5(2)	89.09(14)	
7a	OH	1.907(2)	1.928(2)	101.21(9)	120.81(16)	122.8(2)	–4.3(3)	78.48(19)	13.3(2)
7b	OH	1.910(2)	1.926(2)	101.97(9)	121.12(16)	122.8(2)	7.0(3)	–78.52(19)	–37.0(2)
8	OMe	1.9174(18)	1.9203(16)	99.87(7)	115.05(12)	114.42(15)	1.23(18)	171.79(12)	78.17(14)
9	Me	1.921(2)	1.920(2)	100.48(8)	121.01(14)	123.26(19)	–4.7(3)	66.58(17)	30.29(18)
Average		1.916(7)	1.923(4)	100.6(10)					

Table 3 Intermolecular hydrogen bonds (Å, °)^a

	D–H ⋯ A	D–H	H ⋯ A	D ⋯ A	D–H ⋯ A
2	O4–H4 ⋯ Se1 ⁱ	0.84	2.6265	3.4426(16)	164.30
	C24–H24 ⋯ O4 ⁱⁱ	0.95	2.4724	3.237(4)	137.55
7	O2a–H2a ⋯ O4b ⁱⁱⁱ	0.84	2.3598	2.896(2)	122.18
	O2b–H2b ⋯ O4a ^{iv}	0.84	2.2312	2.840(2)	129.44
	O4a–H4a ⋯ O2b ⁱ	0.84	1.9567	2.784(2)	168.35
	O4b–H4b ⋯ O2a	0.84	1.9293	2.765(2)	172.73
9	O4–H4 ⋯ Se1 ⁱ	0.84	2.6974	3.5354(17)	175.26
	C3–H3 ⋯ Se1 ⁱ	0.95	2.9798	3.806(2)	146.19
	C13–H13 ⋯ O4 ^r	0.95	2.5286	3.381(3)	149.45

^a Missing su's are due to fixing of the hydrogen atoms during refinement. ⁱ*x*,1 + *y*,*z*ⁱⁱ ½ – *x*,½ + *y*,1 + ½ – *z*ⁱⁱⁱ – *x*,1 – *y*,2 – *z*^{iv} – *x*,1 – *y*,1 – *z*^v 1 + *x*, –1 + *y*,*z*.

around 3.5 Å. A short C3–H3 ⋯ Se1 intermolecular contact is also seen in **9**, with an elongation of the donor–acceptor distance relative to the O–Se that matches the difference between O–O and C–O donor–acceptor distances. The packing in **3** and **9** is also stabilised by C–H ⋯ O intermolecular hydrogen bonds.

The orientation of the benzene and phenyl rings relative to each other is a result of rotational freedom around the two selenium bonds. Clearly an *o*-OMe group places a special restraint on the relative orientation of the rings since this is significantly different from what is observed for other *ortho*-substituents. In all the structures investigated, the interplanar angle between the benzene and phenyl ring planes is, however, around 77° and appears to be unaffected by the substitution on the benzene ring. The abundance of this close-to-perpendicular orientation of the two rings could suggest that it corresponds to a minimum in the conformational energy of the isolated molecule.

An inspection of Table 2 reveals that in the systems without *o*-OMe groups, the C2–C1–Se–C11 torsion angles vary less than the C1–Se–C11–C12 torsion angles. It should be noted that the sign is unimportant for the C2–C1–Se–C11 torsion, while it is of importance for C1–Se–C11–C12, as it tells whether C12 and H12 are twisted towards or away from the *ortho*-substituent. This suggests that the barrier for rotation around the Se–C1 bond is higher than for the rotation around Se–C11 bond. Based on these results we would expect that the C2–C1–Se–C11 torsion angles reflect the geometry in solution, while the C1–Se–C11–C12 torsion angles show more variation.

Molecular geometries. The nine structures show the same feature of the Se–C1 distances being significantly shorter than the Se–C11 distances, which average to 1.923(4) Å with small and unsystematic variations. This may reflect that the substituents also influence the Se–C1 distance.

Substituents introduce deviations from the idealised 120° angles of the isolated benzene molecule, and the effects have

been shown to be additive if additional substituents are introduced.¹⁰ We have examined the variations in the angles of the benzene ring observed in compounds **1–9**, to determine whether these could be seen to result from substitution effects. Naming the angles of the ring *a*, *β*, *γ* and *δ*, starting with *a* at the substituted carbon atom, the angle deformations can be described by $\Delta a = a - 120^\circ$, $\Delta \beta = \beta - 120^\circ$ etc. We have determined the substituent effect of the SePh group from the geometrical information of the crystal structures, assuming that effects of the central benzene ring on the phenyl ring of the SePh group is independent of the substituents on the benzene ring. A validation of the assumption leading to the substituent effects can be carried out. From tabulated substitution effects (for ethoxy methoxy is used) and the fact that the effects are additive, the angle deviations in the central benzene rings are calculated. As shown in Fig. 6, the observed deviations from 120° fit nicely to the calculated values based on the following angular substituent effect of a SePh group:

$$\Delta a = 0.14 \pm 0.06^\circ, \Delta \beta = -0.36 \pm 0.04^\circ, \Delta \gamma = 0.45 \pm 0.04^\circ, \text{ and } \Delta \delta = -0.26 \pm 0.06^\circ.$$

An intramolecular interaction between Se and the substituent in the *ortho*-position is observed in all the structures (Tables 4 and 5). This explains why the greatest variations in molecular geometry (Table 2) are found in the selenium surroundings and depend on the nature of the *ortho*-substituent.

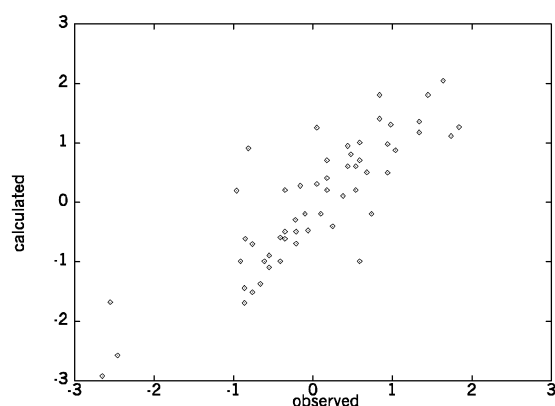
o-OH leads to the formation of an O2–H2 ⋯ Se1 intramolecular hydrogen bond with a O2 ⋯ Se1 distance of 3.1–3.2 Å and an angle of 120–125°. The Se1–C1 distance is considerably below average, while the C1–Se1–C11 angle is larger than 101°.

When a methyl group is situated next to the SePh substituent, the resulting C ⋯ Se distance is approximately 3.2 Å. In **2** a C–H ⋯ Se contact of hydrogen bonding nature is found. The geometry is very similar to what was found for *o*-OH,

Table 4 Intramolecular hydrogen bonds (Å, °)^a

	D–H ⋯ A	D–H	H ⋯ A	D ⋯ A	D–H ⋯ A
1	O2–H2 ⋯ Se1	0.84	2.6157	3.154(2)	123.05
2	C7–H71 ⋯ Se1	0.98	2.7036	3.261(2)	116.51
	C8–H82 ⋯ O4	0.98	2.3047	2.777(3)	108.62
3	O2–H2 ⋯ Se1	0.84	2.6058	3.139(2)	122.63
	O4–H4 ⋯ Se2	0.84	2.5606	3.121(2)	125.17
7	O2a–H2a ⋯ Se1a	0.84	2.6099	3.1528(17)	123.55
	O2b–H2b ⋯ Se1b	0.84	2.6294	3.1701(17)	123.40

^a Missing su's are due to fixing of the hydrogen atoms during refinement.

**Fig. 6** Angle deviations in the central benzene rings calculated from substituent effects plotted against observed deviations.

though the C–H ⋯ Se interaction would be expected to be considerably weaker (longer H ⋯ Se distance and smaller C–H ⋯ Se angle). The *ortho*-contacts in **6** and **9** do not involve hydrogen atoms.

Compound **6** has methyl groups in both *ortho*-positions, the Se1–C1 bond is extremely long and the two ring planes are perpendicular, probably due to the presence of two bulky *ortho*-substituents rather than to the actual nature of the substituents.

The conformational effects exerted by a methoxy group in the *ortho*-position differ from those caused by *o*-OH and *o*-Me substitution. A O2 ⋯ Se1 close contact of 2.8–2.9 Å can be observed. The atoms C11, Se1, O2 and C7 (connected to O2) are all coplanar with the benzene ring with O2 and Se1 bending slightly towards each other. The C2–O2–C7 angle is 117–118° in accordance with the sp² hybridisation of the oxygen atom. The oxygen lone pair therefore lies in the benzene plane as does the C11–Se1 antibonding orbital. Even though the lone pair does not point directly towards the antibonding orbital, some interaction might take place.

In **4** two SePh groups are situated *ortho* to each other. Here a Se1 ⋯ Se2 close contact of 3.4753(11) Å is observed. This is obtained through a lengthening of the Se1–C1 and Se2–C2 bonds and a decrease in the angles around the selenium atoms. The C2–C1–Se1–C11 and C1–C2–Se2–C21 torsion angles bring one phenyl group on each side of the benzene plane.

Relations between the molecular structures and NMR chemical shifts

The crystal structures of compounds **1–9** make it clear that each type of *ortho*-substituent gives rise to a specific interaction with the neighbouring selenium atom. Since the selenium contacts are intramolecular, the interactions are likely to be found in solution as well, and can thus be used to explain the effects of the *ortho*-substituents on the ⁷⁷Se NMR chemical shifts.

The structures of **1**, **3** and **7** show that the contact to a neighbouring OH group is mediated through a hydrogen bond. This fact offers an explanation of the two apparent discrepancies in the NMR series. With an alternative and stronger hydrogen

bond acceptor situated at the other side of OH, the shielding exerted by this group decreases to the same range as found for OMe groups (entry 17) indicating a change from hydrogen bonding to Se ⋯ O contact. When an OH group is situated between two SePh groups (entries 27, 29, 32, 40) the shielding of both selenium atoms decreases to ~100 ppm. This value is consistent with a situation of rapid exchange on the NMR time scale such that each selenium atom experiences an average of a hydrogen bond and an oxygen shielding effect.

In addition to the large shielding effects caused by close encounters between selenium and hydrogen or a 2nd row element (oxygen), Table 1 reveals another systematic trend. The presence of an additional SePh substituent on the ring always has a deshielding effect. The effects are considerable (+25–40 ppm) in the case of close *ortho*-contacts (entries 2, 4), while they are more variable for *m*-SePh. Small (< +10 ppm) effects are seen with a hydrogen atom in the intervening position (e.g. entry 8 vs. 13). Much larger effects (+35 ppm) are encountered when a Me group is inserted between the two selenium atoms (entries 21, 28, 31). This difference suggests that the observed deshielding is in some way transmitted by a dispersion effect, which can be mediated through the close contacts to an intervening Me group.

The idea that a methyl group can function as a relay between two selenium atoms receives some support from the ¹H NMR shifts. The Me signals are observed at 2.2 ± 0.1 ppm for groups with no SePh neighbour, at 2.4 ± 0.1 ppm for groups with one SePh neighbour and at 2.8 ± 0.05 ppm for groups with two SePh neighbours. Thus the deshielding exerted by two adjacent selenium atoms is distinctly larger than twice the contribution from a single selenium atom.

The two bromine substituted compounds (entries 6, 16) show the same trend as seen for selenium. This suggests that the ⁷⁷Se deshielding observed in the present study may be a common property for 4th row elements. In this context it is notable that a 3rd row element (chlorine) has a negligible *ortho*-effect (< 5 ppm shielding; entries 9 vs. 8 and 15 vs. 13).

While δ ⁷⁷Se seems to be little affected by the relative orientations of phenyl and benzene rings (seeing that *o*-Me and *o*-OMe give rise to very different orientations of the two rings, but similar ⁷⁷Se chemical shifts), the reverse is true of the effect of the SePh substituent on the chemical shifts of neighbouring protons. The signal from the proton *ortho* to a SePh group with a Me or OH neighbour (C2–C1–Se–C11: 67–82°) appears at 7.60–7.34 ppm while that from the proton *ortho* to a SePh group with an OMe neighbour (C2–C1–Se–C11: 162–176°) appears at 7.1–6.5 ppm. The existence of a correlation between the shifts of protons *ortho* to SePh and the C2–C1–Se–C11 torsional angles observed in the crystal structures indicates that this structural feature is not a fortuitous result of crystal packing, but also present in the solvated molecule as argued earlier.

The polarization of the ¹H NMR shifts in the phenylselenium substituent is also affected by the C2–C1–Se–C11 torsional angles. In SePh groups *ortho* to an OH or Me group all five protons appear as an, eventually slightly broadened, singlet. In SePh groups *ortho* to OMe the *ortho*-protons are distinctly

Table 5 Intramolecular close contacts (Å, °)

Contact	Sum of van der Waals radii/Å	Distance/Å
1 Se2 ... O4	3.42	2.910(2)
4 Se1 ... Se2	3.80	3.4753(11)
O4 ... O5	3.04	2.586(3)
5 Se1 ... O2	3.42	2.818(2)
6 Se1 ... C7	3.60	3.195(2)
Se1 ... C9	3.60	3.186(2)
8 Se1 ... O2	3.42	2.8212(13)
9 Se1 ... C7	3.60	3.241(2)

deshielded and appear as a multiplet 0.2 ppm downfield from the multiplet of *meta*- and *para*-signals. The situation for two adjacent phenylseleno groups is less clear cut. In the spectrum of 1,2-diethoxy-4,5-bis(phenylseleno)benzene (structure 4, entry 4) the proton signals from both SePh groups are polarized and the protons on the central ring are shielded (6.80 ppm). In that of 1-methoxy-2,6-dimethyl-3,4-bis(phenylseleno)benzene (entry 2) one SePh group shows a singlet, the other multiplets of 2 and 3H. For this compound the proton on the central ring is also deshielded (6.60 ppm).

Conclusions

Analysis of the crystal structures provided solid evidence for the assumption that the through-space interactions between selenium and the *ortho*-substituent(s) observed in the solid state are also likely to be present in solution. The structural parameters displayed in Table 2 reflect these interactions, except for the invariant Se–C11 bond length and the C1–Se–C11–C12 torsional angle, which could be influenced by crystal packing.

The variations in ^{77}Se NMR chemical shifts can be explained from the intramolecular interactions with the *ortho*-substituents. These *ortho*-effects are roughly additive and are affected in the expected way when the *ortho*-substituent is able to engage in other/simultaneous interactions. Thus the actual interactions and not just their conformational constraints on the selenium surroundings are the reason for the variations in δ ^{77}Se .

The conformational changes resulting from the interactions to the *ortho*-substituents are, however, reflected in the ^1H NMR chemical shifts of the *ortho*-proton and the protons on the phenylseleno substituent. Especially the relative orientation of the phenyl and benzene rings, described by the C2–C1–Se–C11 torsional angle, are of importance.

Experimental

NMR spectra, in CDCl_3 , 298 K, were recorded on a Varian Mercury 300 MHz instrument (^{77}Se resonance at 57.3 MHz) or a JEOL FX 90 Q instrument (^{77}Se resonance at 17.1 MHz). ^{77}Se chemical shifts are given relative to Me_2Se in CDCl_3 , ^1H shifts relative to TMS as internal standard.

C, H microanalyses (C: $\pm 0.15\%$; H: $\pm 0.10\%$) were performed in-house.

Melting points were determined by means of a Büchi melting point microscope.

Preparations

General procedures. Procedures A–C are *para*-selective reactions. Procedure A is the mildest one and preferred for phenolic substrates. Procedure B is the general choice for anisoles with a free *para*-position while the more forcing procedure C is applied to anisoles with *para*- and/or deactivating substituents. The relative reaction rates toward anisole are $A : B : C = 1 : 25 : 1500$. Procedure D is applied for *ortho*-specific substitution of phenols.⁵

A. A solution of dihydroxyphenylselenonium *p*-toluenesulfonate¹¹ (1 mmol), diphenyl diselenide¹¹ (1 mmol) and the

appropriate arene (3.1 mmol, or 1.6 mmol in case of intended disubstitution) in methanol–20% dichloromethane (5 ml) is stirred at room temperature until TLC (silica gel 60/dichloromethane–8% methanol) shows no spot from benzeneseleninic acid ($R_f \approx 0.4$). The reaction mixture is diluted with water and extracted with pentane containing 0–10% dichloromethane. Phenols are extracted from this solution with 2 M NaOH and, following acidification, reextracted with pentane containing 0–10% dichloromethane. The extract is evaporated and the residue recrystallized as given for the individual compounds. Neutral products (anisoles) are crudely purified by flash chromatography (silica gel 60/pentane–10–40% dichloromethane) prior to recrystallization.

B. As method A, but in methanol, 65 °C.

C. As method A, but in acetic acid, 100–110 °C.

D. *o*-(Phenylseleno)phenols with a free *para*-position are prepared in the unavoidable⁵ mixture with the *p*-quinone and (phenylseleno)quinones by mixing benzeneseleninic acid (1.5 mmol), diphenyl diselenide, (1 mmol) and the parent phenol (3 mmol) in a small test tube. A fast exothermic reaction starts spontaneously or is initiated by gentle heating. The product mixture is diluted with dichloromethane–25% pentane and filtered through silica gel 60 (3 g), washing the filter with another 15 ml of solvent. The filtrate is extracted with 2 M NaOH (3 \times 3 ml). The aqueous phase is acidified and extracted with pentane–20% dichloromethane (2 \times 10 ml). This extract is filtered through silica gel 60 (6 g), washing the filter with an additional 20 ml of the same solvent. The filtrate is evaporated and the residue recrystallized as given for the individual compounds.

Compounds. (Structures, see Fig. 1; ^{77}Se NMR data, Table 1.) *p*-Nitrophenyl phenyl selenide (entry 1): ref. 7.

1-Methoxy-2,6-dimethyl-3,4-bis(phenylseleno)benzene (entries 2, 22): From 1-methoxy-2,6-dimethylbenzene, method C, 45 min, yield 50%, mp 85–86 °C (MeOH), $\text{C}_{21}\text{H}_{20}\text{OSe}_2$ (C,H), M^+ 448 ($^{80}\text{Se}_2$), ^1H NMR (ppm): 7.65–7.57, m, 2H; 7.40–7.30, m, 3H; 7.20, s, 5H, 6.60, s, 1H; 3.63, s, 3H, 2.39, s, 3H; 2.12, s, 3H.

2-Hydroxy-3,5-bis(phenylseleno)benzoic acid (entries 3, 17): From salicylic acid, method B, 20 h, yield 30%, mp 167–169 °C (wet methanol), $\text{C}_{19}\text{H}_{14}\text{O}_3\text{Se}_2$ (C,H), M^+ 450 ($^{80}\text{Se}_2$), ^1H NMR (ppm): 10.1, s, 1H; 8.8, s, 1H; 7.98, d, 1H; 7.58–7.45, m, 2H; 7.4–7.2, m, 9H.

1,2-Diethoxy-4,5-bis(phenylseleno)benzene (structure; entry 4): From 1,2-diethoxybenzene, method A, 3 days, yield 90%, mp 88–89 °C (hexane) 91–92 °C (MeOH). $\text{C}_{22}\text{H}_{22}\text{O}_2\text{Se}_2$ (C,H), M^+ 478 ($^{80}\text{Se}_2$), ^1H NMR (ppm): 7.5–7.4, m, 4H; 7.3–7.2, m, 6H; 6.80, s, 2H; 3.87, q, 4H; 1.38, t, 6H.

2-Bromo-1-methoxy-4-(phenylseleno)benzene (entry 6): From *o*-bromoanisole, method C, 1 h, yield 67%, mp 87–89 °C (MeOH), $\text{C}_{13}\text{H}_{11}\text{BrOSe}$ (C,H), M^+ 342 ($^{78}\text{Se}^{81}\text{Br} + ^{80}\text{Se}^{79}\text{Se}$). ^1H NMR (ppm): 7.72, d (2 Hz), 1H; 7.45, dd (8 + 2 Hz), 1H; 7.35–7.15, m, 5H; 6.80, d (8 Hz), 1H; 3.86, s, 3H.

2-Hydroxy-5-(phenylseleno)benzaldehyde (entry 7): From 2-hydroxybenzaldehyde, method A, 6 days, yield 59%, mp 53–54 °C (pentane), $\text{C}_{13}\text{H}_{10}\text{O}_2\text{Se}$ (C,H), M^+ 278 (^{80}Se). ^1H NMR (ppm): 11.84, s, 1H; 9.82, s, 1H; 7.76, d (2 Hz), 1H; 7.70, dd (2+9 Hz), 1H; 7.45–7.20, m, 5H; 6.94, d (9 Hz), 1H.

2,4-Bis(phenylseleno)phenol (entries 8,36): By-product from 4-(phenylseleno)phenol, by chromatography of mother liquor, mp 72–74 °C (pentane), $\text{C}_{18}\text{H}_{14}\text{OSe}_2$ (C,H), M^+ 406 ($^{80}\text{Se}_2$). ^1H NMR (ppm): 7.86, d (2 Hz), 1H; 7.51, dd (2 + 9 Hz), 1H; 7.35–7.10, m, 5H; 7.18, s, 5H; 6.97, d (9 Hz), 1H; 6.47, s, 1H.

3-Chloro-4,6-bis(phenylseleno)phenol (entries 9, 33): By-product from 3-chloro-4-(phenylseleno)phenol, isolated by chromatography (silica gel 60/hexane–40% dichloromethane), mp 81–83 °C (pentane), $\text{C}_{18}\text{H}_{13}\text{ClOSe}_2$ (C,H), M^+ 440 ($^{35}\text{Cl}^{80}\text{Se}$). ^1H NMR (ppm): 7.53, s, 1H; 7.45–7.40, m, 2H; 7.30–7.25, m, 3H; 7.19, s, 5H; 6.38, s, 1H.

2-Methyl-4-(phenylseleno)phenol (entry 10): From 2-methylphenol, method A, 1 h, yield 76%, mp 59–60 °C, C₁₃H₁₂OSe (C,H), M⁺ 264 (⁸⁰Se). ¹H NMR (ppm): 7.40–7.15, m, 7 H; 6.70, d (8 Hz), 1H, 4.86, s, 1H; 2.21, s, 3H.

2,6-Dimethyl-4-(phenylseleno)phenol (entry 11): From 2,6-dimethylphenol, method A, 1 h, yield 37%, mp 29–30 °C (pentane), C₁₄H₁₄OSe (C,H), M⁺ 278 (⁸⁰Se). ¹H NMR (ppm): 7.35–7.12, m, 7H; 4.73, s, 1H; 2.19, s, 6H.

1-Methoxy-4-(phenylseleno)benzene (entry 12): ref. 5.

4-(Phenylseleno)phenol (entry 13): ref. 5.

1-Methoxy-2-methyl-4-(phenylseleno)benzene (entry 14): From 2-methylanisole, method C, 10 min, yield 92%, mp 57–58 °C (pentane), C₁₄H₁₄OSe (C,H), M⁺ 278 (⁸⁰Se). ¹H NMR (ppm): 7.43, dd (2+8 Hz), 1H; 7.39, d (2 Hz), 1H; 7.35–7.31, m, 2H; 7.25–7.17, m, 3H; 6.78, d (8 Hz), 1H; 3.82, s, 3H; 4.41, s, 3H.

3-Chloro-4-(phenylseleno)phenol (entry 15): From 3-chlorophenol, method B, 1 h, yield 55%, oil, purified by chromatography (silica gel 60/hexane–75% dichloromethane). ¹H NMR (ppm): 7.48–7.40, m, 2H; 7.35–7.20, m, 3H; 7.08, d (9 Hz), 1H; 6.91, d (2 Hz), 1H, 6.57, dd (9+2 Hz), 1H; 5.24, s, 1H.

4-Bromo-1-methoxy-2-(phenylseleno)benzene (entry 16): From 4-bromoanisole, method C, 90 min, yield 22%, mp 92–93 °C (MeOH), C₁₃H₁₁BrOSe (C,H), M⁺ 342 (⁷⁸Se⁸¹Br + ⁸⁰Se⁷⁹Br). ¹H NMR (ppm): 7.65–7.55, m, 2H; 7.40–7.30, m, 3H; 7.25, dd (8+2 Hz), 1H; 6.21, d (2 Hz), 1H; 6.68, d (8 Hz), 1H; 3.85, s, 3H.

2,3-Dimethyl-4-(phenylseleno)phenol (structure 2, entry 18): From 2,3-dimethylphenol, method A, 50 min, yield 75%, mp 72–73 °C (hexane), C₁₄H₁₄OSe (C,H), M⁺ 278 (⁸⁰Se). ¹H NMR (ppm): 7.36, d (8 Hz), 1H; 7.21, s, 5H; 5.56, d (8 Hz), 1H; 5.10, s, 1H; 2.41, s, 3H; 2.22, s, 3H.

1,4-Dimethoxy-2,5-bis(phenylseleno)benzene (structure 5, entry 19): From 1,4-dimethoxybenzene, method C, yield 64%, mp 177–179 °C, C₂₀H₁₈O₂Se₂ (C,H), M⁺ 450 (⁸⁰Se₂). ¹H NMR (ppm): 7.60–7.50, m, 4H; 7.40–7.25, m, 6H; 6.54, s, 2H; 3.58, s, 6H.

1-Methoxy-4-methyl-2-(phenylseleno)benzene (structure 8, entry 20): From 4-methylanisole, method B, 24 h, yield 79%, mp 71–73 °C (pentane), C₁₄H₁₄OSe (C,H), M⁺ 278 (⁸⁰Se). ¹H NMR (ppm): 7.60–7.55, m, 2H; 7.35–7.30, m, 3H; 7.00, dd (1.5+8 Hz), 1H; 6.84, d (1.5 Hz), 1H; 6.77, d (8 Hz), 1H; 3.86, s, 3H; 2.17, s, 3H.

3,5-Dimethyl-2,4,6-tris(phenylseleno)phenol (entries 21, 32): From 3,5-dimethyl-4-(phenylseleno)phenol, method A, 4 days, yield 37%, mp 175–177 °C (dichloromethane–hexane), C₂₆H₂₂OSe₃ (C,H), M⁺ 588 (⁷⁸Se⁸⁰Se₂). ¹H NMR (ppm): 7.55, s, 1H; 7.16, s, 15H; 2.84, s, 6H.

1,3-Dimethoxy-4,6-bis(phenylseleno)benzene (entry 23): From 1,3-dimethoxybenzene, method A, 24 h, yield 87%, mp 91–92 °C (dichloromethane–hexane), C₂₀H₁₈O₂Se₂ (C,H), M⁺ 450 (⁸⁰Se₂). ¹H NMR (ppm): 7.35–7.25, m, 4H; 7.20–7.10, m, 6H; 7.06, s, 1H; 6.46, s, 1H; 3.81, s, 6H.

4,6-Bis(phenylseleno)-3-methoxyphenol (structure 1, entries 24, 42): From 3-methoxyphenol, method A, 10 min, yield 49%, mp 78–80 °C, C₁₉H₁₆O₂Se₂ (C,H), M⁺ 436 (⁸⁰Se₂). ¹H NMR (ppm): 7.57, s, 1H; 7.30–7.35, m, 2H; 7.25–7.15, m, 3H; 7.14, s, 5H, 6.64, s, 1H; 6.51, s, 1H; 3.81, s, 3H.

2,5-Dimethyl-4-(phenylseleno)phenol (structure 9, entry 25): From 2,5-dimethylphenol, method A, 15 min, yield 89%, mp 63–64 °C, C₁₄H₁₄OSe (C,H), M⁺ 278 (⁸⁰Se). ¹H NMR (in DMSO-d₆) (ppm): 9.63, s, 1H; 7.34, s, 1H; 7.25–7.12, m, 5H; 6.83, s, 1H; 2.25, s, 3H; 2.09, s, 3H.

1,3-Dimethoxy-4-(phenylseleno)benzene (entry 26): From 1,3-dimethoxybenzene, method A, 24 h, yield 59%, mp 28–29 °C, C₁₄H₁₄O₂Se (C,H), M⁺ 294 (⁸⁰Se). ¹H NMR (ppm): 7.45–7.30, m, 2H; 7.25–7.15, m, 4H; 6.48, d (2 Hz); 1H; 6.41, dd (2+8 Hz), 1H; 3.80, s, 3H; 3.78, s, 3H.

Methyl 4-hydroxy-3,5-bis(phenylseleno)benzoate (entry 27): From methyl 4-hydroxybenzoate, method B, 4 days, yield 66%, mp 103–104 °C (hexane), C₂₀H₁₆O₃Se₂ (C,H), M⁺ 464 (⁸⁰Se₂). ¹H

NMR (ppm): 8.04, s, 2H; 7.45–7.25, m, 10H, 7.22, s, 1H, 3.78, s, 3H.

3,5-Dimethyl-2,4-bis(phenylseleno)phenol (entries 28, 44): By-product (2%) in the preparation of 3,5-dimethyl-4-(phenylseleno)phenol (entry 33), mp 100–101 °C (hexane), C₂₀H₁₈OSe₂ (C,H), M⁺ 434 (⁸⁰Se₂). ¹H NMR (ppm): 7.20–7.10, m, 5H; 7.17, s, 5H; 7.02, s, 1H, 9.92, s, 1H, 2.74, s, 3H; 2.51, s, 3H.

2,6-Bis(phenylseleno)phenol (entry 29): From phenol, method D, yield 37%, mp 59–61 °C (pentane), C₁₈H₁₄OSe₂ (C,H), M⁺ 406 (⁸⁰Se₂). ¹H NMR (ppm): 7.47–7.20, m, 12H; 6.85, s, 1H; 6.72, t (7.5 Hz), 1H.

1-Methoxy-3,5-dimethyl-4-(phenylseleno)benzene (structure 6, entry 30): From 3,5-dimethylanisole, method A, 3 days, yield 79%, mp 82–84 °C (pentane), C₁₅H₁₆OSe (C,H), M⁺ 292 (⁸⁰Se). ¹H NMR (ppm): 7.09, s, 5H; 6.73, s, 2H; 3.79, s, 3H; 2.45, s, 6H.

3,5-Dimethyl-4-(phenylseleno)phenol (entry 31): From 3,5-dimethylphenol, method A, 2 h, yield 76%, mp 91–92 °C (hexane), C₁₄H₁₄OSe (C,H), M⁺ 278 (⁸⁰Se). ¹H NMR (ppm): 7.09, s, 5H; 6.66, s, 2H; 5.29, s, 1H; 2.40, s, 6H.

Methyl 4-hydroxy-3-(phenylseleno)benzoate (entry 34): Byproduct (6%) in the preparation of methyl 4-hydroxy-3,5-bis(phenylseleno)benzoate (entry 29), mp 88–89 °C (hexane), C₁₄H₁₂O₃Se (C,H), M⁺ 308 (⁸⁰Se). ¹H NMR (ppm): 8.35, d (2 Hz), 1H; 8.02, dd (2 +10 Hz), 1H; 7.22, s, 5H; 7.06, d (10 Hz); 1H; 6.94, s, 1H; 3.87, s, 3H.

4-Methyl-2-(phenylseleno)phenol (entry 35): From 4-methylphenol, method B, 30 min, oil, C₁₃H₁₂OSe (C,H), M⁺ 264 (⁸⁰Se). ¹H NMR (ppm): 7.34, d (2 Hz), 1H; 7.19, s, 5H; 7.14, dd (2 +8 Hz), 1H; 6.95, d (8 Hz), 1H; 6.25, s, 1H; 2.26, s, 3H.

2-(Phenylseleno)phenol (entry 37): From phenol, method D, yield 40%, oil, C₁₂H₁₀OSe (C,H), M⁺ 250 (⁸⁰Se). ¹H NMR (ppm): 7.60, dd (2+8 Hz), 1H; 7.33, dt (2+8 Hz), 1H; 7.18, s, 5H; 7.05, dd (2+8 Hz), 1H; 6.85, dt (2+8 Hz), 1H; 4.73, s, 1H.

2-Methyl-6-(phenylseleno)phenol (entry 38): From 2-methylphenol, method D, yield 31%, mp 29–30 °C (pentane), C₁₃H₁₂OSe (C,H), M⁺ 264 (⁸⁰Se). ¹H NMR (ppm): 7.47, dd (1.5+8 Hz), 1H; 7.19, s-br., 6H; 6.78, t (8 Hz), 1H; 6.52, s, 1H; 2.29, s, 3H.

3-Chloro-6-(phenylseleno)phenol (entry 39): From 3-chlorophenol, method D, yield 10%, mp 35–36 °C (pentane), C₁₂H₉ClOSe (C,H), M⁺ 284 (³⁵Cl⁸⁰Se). ¹H NMR (ppm): 7.53, d (8 Hz), 1H; 7.19, s, 5H, 7.13, d (2 Hz); 1H; 6.99; dd (2+8 Hz), 1H; 6.47, s, 1H.

3,5-Dimethyl-2,6-bis(phenylseleno)phenol (entry 40): From 3,5-dimethylphenol, method D, yield 67%, mp 119–121 °C (hexane), C₂₀H₁₈OSe₂ (C,H), M⁺ 434 (⁸⁰Se₂). ¹H NMR (ppm): 7.23, s, 1H; 7.16, s, 5H; 9.91, s, 1H; 2.46, s, 6H.

4,6-Bis(phenylseleno)benzene-1,3-diol (structure 3, entry 41): From 4-(phenylseleno)benzene-1,3-diol, method A, 15 min, yield 56%, mp 121–122 °C (dichloromethane–hexane), C₁₈H₁₄O₂Se₂ (C,H), M⁺ 422 (⁸⁰Se₂). ¹H NMR (ppm): 7.96, s, 1H; 7.19, s, 10H; 6.82, s, 1H; 6.62, s, 2H.

4-(Phenylseleno)benzene-1,3-diol (structure 7, entry 43): From benzene-1,3-diol, method A, 30 min, yield 35%, mp 112–113 °C (dichloromethane–pentane), C₁₂H₁₀O₂Se (C,H), M⁺ 266 (⁸⁰Se). ¹H NMR (ppm): 7.50, d (8 Hz), 1H; 7.18, s, 5H; 6.58, d (2 Hz), 1H; 6.50, s, 1H; 6.41, dd (2+8 Hz), 1H; 5.32, s, 1H.

3,5-Dimethyl-2-(phenylseleno)phenol (entry 45): From 3,5-dimethylphenol, method D, yield 40%, mp 58–59 °C (pentane), C₁₄H₁₄OSe (C,H), M⁺ 278 (⁸⁰Se). ¹H NMR (ppm): 7.14, s, 5H; 6.76, s, 1H; 6.70, s, 1H; 6.67, s, 1H; 2.39, s, 3H; 2.30, s, 3H.

X-Ray crystallography

Single crystal data were collected on crystals cooled to 122.0(5) K on an Enraf-Nonius CAD4 diffractometer.¹² The employed radiation was obtained from a graphite monochromator. Data reductions were performed with the DREADD package.¹³ All reflections were corrected for background, Lorentz and polarisation effects. The data sets were scaled to account for the

Table 6 Crystal data, data collection and refinement

	1	2	3	4	5	6	7	8	9
Formula	C ₁₉ H ₁₆ O ₂ Se ₂	C ₁₄ H ₁₄ OSe	C ₁₈ H ₁₄ O ₂ Se ₂	C ₂₂ H ₂₂ O ₂ Se ₂	C ₂₀ H ₁₈ O ₂ Se ₂	C ₁₅ H ₁₆ OSe	C ₁₂ H ₁₀ O ₂ Se	C ₁₄ H ₁₄ OSe	C ₁₄ H ₁₄ OSe
M _r /g mol ⁻¹	434.24	277.21	420.21	476.32	448.26	291.24	265.16	277.21	277.21
Crystal system	Monoclinic	Triclinic	Monoclinic	Triclinic	Monoclinic	Monoclinic	Triclinic	Orthorhombic	Monoclinic
Space group	<i>P</i> 2 ₁ / <i>c</i>	<i>P</i> 1	<i>P</i> 2 ₁ / <i>n</i>	<i>P</i> 1	<i>P</i> 2 ₁ / <i>c</i>	<i>P</i> 2 ₁ / <i>n</i>	<i>P</i> 1	<i>Pbca</i>	<i>P</i> 2 ₁ / <i>c</i>
<i>a</i> /Å	10.516(4)	7.2242(15)	15.0339(15)	8.5958(17)	7.1618(10)	7.2789(7)	8.7061(11)	14.991(2)	9.0416(12)
<i>b</i> /Å	18.569(6)	7.9556(11)	5.6420(7)	11.370(3)	15.1320(19)	9.4958(8)	10.3054(8)	9.9673(18)	7.8911(10)
<i>c</i> /Å	8.832(4)	11.007(2)	18.9279(13)	12.388(3)	8.2912(10)	19.043(3)	11.8008(13)	15.930(2)	17.6103(18)
<i>α</i> /°	90.00	83.594(14)	90.00	116.25(2)	90.00	90.00	92.369(8)	90.00	90.00
<i>β</i> /°	100.21(4)	73.236(16)	101.673(7)	100.280(17)	103.609(11)	97.047(11)	90.070(10)	90.00	102.406(10)
<i>γ</i> /°	90.00	86.000(14)	90.00	104.48(2)	90.00	90.00	94.027(9)	90.00	90.00
<i>V</i> /Å ⁻³	1697.5(12)	601.5(2)	1572.3(3)	991.4(4)	873.31(19)	1306.3(3)	1055.24(19)	2380.3(6)	1227.1(3)
<i>Z</i>	4	2	4	2	2	4	4	8	4
<i>D</i> /g cm ⁻¹	1.699	1.531	1.775	1.596	1.705	1.481	1.669	1.547	1.500
Data collection									
<i>T</i> /K	122.0(5)	122.0(5)	122.0(5)	122.0(5)	122.0(5)	122.0(5)	122.0(5)	122.0(5)	122.0(5)
Radiation	CuKα	CuKα	CuKα	CuKα	CuKα	CuKα	CuKα	CuKα	MoKα
<i>λ</i> /Å	1.5418	1.5418	1.5418	1.5418	1.5418	1.5418	1.5418	1.5418	0.71073
<i>μ</i> /mm ⁻¹	5.497	4.014	5.911	4.761	5.363	3.724	4.622	4.057	3.035
<i>θ</i> -range/°	4.27–74.90	4.21–74.85	3.44–74.91	4.22–74.91	5.85–74.93	4.68–74.91	3.75–74.87	5.55–74.91	2.31–26.43
Refinement									
Total refl.	7508	4817	6277	6745	4116	6618	11170	6046	9405
<i>R</i> _{int}	0.0232	0.0489	0.0473	0.0290	0.0451	0.0422	0.0273	0.0315	0.0501
Unique refl.	3478	2454	3226	3936	1797	2676	4334	2447	2520
Parameters	211	148	202	227	111	158	276	148	149
Ext. coeff.	0.00274(14)	—	0.00456(17)	—	0.0082(7)	0.0046(2)	0.0092(3)	0.00204(8)	0.0075(8)
<i>R</i> ₁ ^a	0.0325	0.0250	0.0302	0.0355	0.0352	0.0262	0.0292	0.0266	0.0268
<i>wR</i> ₂ ^a	0.0804	0.0678	0.0838	0.0867	0.0965	0.0697	0.0783	0.0727	0.0760
GoF	1.076	1.134	1.224	1.094	1.104	1.065	1.115	1.153	1.100

^a All data.

intensity decrease during exposure time. Absorption corrections were performed using a Gaussian integration procedure.¹⁴ Crystallographic data for the compounds are summarized in Table 6.

The structures were solved by Patterson and Fourier methods using SHELXS-97.¹⁵ Refinements against all *F*_o²-values were carried out using SHELXL-97.¹⁶ The heavy (non-hydrogen) atoms were refined with anisotropic displacement parameters. The hydrogen atoms were positioned using standard distances and angles. For OH and Me groups the torsional orientations were refined. The isotropic displacement parameters for the hydrogen atoms were fixed to be 1.2 and 1.5 times that of the parent atom for hydrogen bonded to carbon and oxygen atoms, respectively. At the end of the refinements the standard weights were replaced by the weighting scheme suggested by the program, and an extinction parameter was refined if the data indicated extinction. The results from the refinements are listed in Table 6.

Acknowledgements

We wish to thank Mrs Karin Linthoe, Laboratory of Organic Chemistry, for carrying out the micro analysis, and Mr Flemming Hansen, Centre of Crystallographic Studies, for help with crystallographic experiments.

References

- S. Gronowitz, A. Konar and A.-B. Hörnfeld, *Org. Magn. Reson.*, 1977, **9**, 213–217.
- W. McFarlan and R. J. Wood, *J. Chem. Soc., Dalton Trans.*, 1972, **35**, 1397.
- H. Duddeck, *Prog. Nucl. Magn. Reson. Spectrosc.*, 1995, **27**, 1–323.
- E. G. Hope, T. Kemmitt and W. Levason, *J. Chem. Soc., Perkin Trans. 2*, 1987, 487–490.
- L. Henriksen, *Tetrahedron Lett.*, 1994, **35**, 7057–7060.
- L. Henriksen and N. Stühr-Hansen, *Phosphorus, Sulfur Silicon Relat. Elem.*, 1998, **136**, 175–190.
- L. Henriksen and N. Stühr-Hansen, *J. Chem. Soc., Perkin Trans. 1*, 1999, 1915–1916.
- C. K. Johnson, ORTEPII, Report ORNL-5138, Oak Ridge National Laboratory, Tennessee, 1976.
- A. L. Spek, PLATON, A Multipurpose Crystallographic Tool, Utrecht University, The Netherlands, 2001.
- A. Dominicano and P. Murray-Rust, *Tetrahedron Lett.*, 1979, **24**, 2283–2286.
- L. Henriksen and N. Stühr-Hansen, *Synth. Commun.*, 1996, **26**, 1897–1902.
- CAD4 Express, Version 5.1, Enraf-Nonius, Delft, The Netherlands, 1994.
- R. H. Blessing, *Crystallogr. Rev.*, 1987, **1**, 3–58.
- G. T. DeTitta, *J. Appl. Crystallogr.*, 1985, **18**, 75–79.
- G. M. Sheldrick, *Acta Crystallogr., Sect. A*, 1990, **46**, 467–473.
- G. M. Sheldrick, SHELXL-97, Program for the Refinement of Crystal Structures, University of Göttingen, Germany, 1997.
- Cerius², Version 3.5, Molecular Simulations Inc., San Diego, 1997.